LOW TEMPERATURE TEST OF A LOW-BETA ELLIPTICAL CAVITY FOR PEFP LINAC EXTENSION*

Han-Sung Kim#, Hyeok-Jung Kwon, Yong-Sub Cho, KAERI, Daejeon, Korea

Abstract

For the future extension of the PEFP (Proton Engineering Frontier Project) proton linac, a study on the SRF technology has been performed including a prototype cavity development to confirm the design of the cavity and fabrication procedures and to check the RF and mechanical properties of a low-beta elliptical cavity. The geometrical beta and resonant frequency of operating mode are 0.42 and 700 MHz, respectively. The cavity is a five-cell structure stiffened by double-ring structure to increase mechanical stability. For the vertical test of the cavity, RF system based on PLL (phase locked loop) has been prepared. If there is no magnetic shielding and operating temperature is 4.2 K, the required RF power to generate the design accelerating field of 8 MV/m is estimated to be about 320 W at critical coupling. In case single RF amplifier cannot deliver sufficient RF power, a coaxial type two-way RF combiner is under consideration. The details of the cavity test setup and results will be presented in this paper.

PEFP LINAC EXTENSION PLAN

The proton linac for PEFP is a 100-MeV machine. To extend the output beam energy up to 1 GeV, SRF technology is under consideration. The overall parameters of the PEFP SRF linac are like followings.

- Input proton energy:	100 MeV
- Output proton energy:	1000 MeV
- Peak beam current:	20 mA
- Beam duty factor:	5 %
- Beam power:	1 MW
- Frequency:	700 MHz
- RF source:	150 kW IOT
- Cavity structure:	Elliptical cavity
- Number of cavity group:	2
- Beam focusing:	SC solenoid

Preliminary study on the beam dynamics shows that two cavity groups (β_g = 0.50 and β_g = 0.74) can provide the required beam energy. The cavity geometrical beta is defined by the cell length of $\beta_g \lambda/2$, where λ is the RF free space wavelength. The operating frequency is determined to be 700 MHz because the operating frequency of the RFQ and DTL is 350 MHz. Beam focusing will be provided by superconducting solenoid magnets installed between every two cavities, which means single cryomodule will host 4 cavities and 2 solenoid magnets.

Figure 1 shows the cavity geometry of two groups. Number of cells per cavity is 6 for both groups. The RF power requirement for each cavity is shown in Fig. 2. An inductive output tube (IOT) is chosen for the RF source due to its low operating voltage and economic reasons. The output RF power of single IOT is limited to about 150 kW, therefore, two IOTs per cavity are going to be used if the required RF power per cavity is more than 150 kW. No cavity requires more than 300 kW.

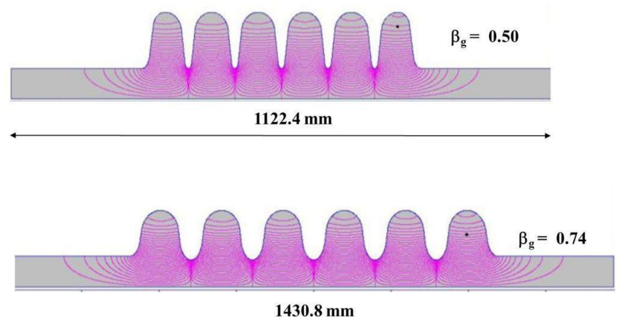

Figure 1: Cavity geometry for PEFP SRF linac.

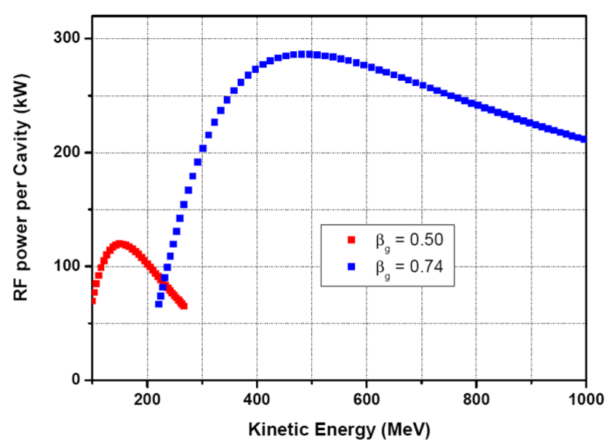

Figure 2: RF power requirement for each cavity.

PROTOTYPE CAVITY

To gain an experience and check the design concept, we developed the prototype cavity which has following design parameters [1].

- Frequency:	700 MHz
- Operating mode:	TM010 PI mode
- Cavity shape:	Elliptical
- Geometrical beta:	0.42
- Number of cells:	5
- Accelerating gradient:	8 MV/m @2.0K
- Epeak/Eacc:	3.71
- Bpeak/Eacc:	7.47 mT/(MV/m)

*Work supported by MEST of the Korean Government.
#kimhs@kaeri.re.kr

- r/Q: 102.3 ohm
- Epeak: 29.68 MV/m
- Field flatness: better than 8.0 %
- Cell to cell coupling: 1.41 %
- Geometrical factor: 121.68 ohm
- Cavity wall thickness: 4.3 mm
- Lorentz force detuning: 0.4 Hz/(MV/m)^2
- Stiffening structure: Double ring structure
- Effective length: 0.45 m

The geometrical beta of the prototype is 0.42, which is lower than that of the PEFP SC linac (0.50) and the number of cell in a prototype cavity is five, not six as for PEFP SC linac. These differences are because the transition energy from normal conducting section to superconducting section used to be 80 MeV, not 100 MeV at the very initial phase.

In an elliptical cavity with a reduced beta, mechanical stabilities are issues to be addressed, especially for a pulsed operation machine. We chose to attach double-ring stiffening structure around dumbbell in center cells to reduce Lorentz force detuning. In addition, the cavity wall thickness is 4.5 mm before chemical processing for better mechanical stability. The ANSYS simulation showed that the Lorentz detuning factor can be as high as 19.2 Hz/(MV/m)^2 with a single-ring stiffening structure, which is unacceptably high. By using double-ring stiffening structure with thick cavity wall, the Lorentz detuning factor can be reduced below 1 Hz/(MV/m)^2.

The diameter of the cavity is about 380 mm and total length including the NbTi flange is about 860 mm. There is no fundamental power coupler port or HOM coupler port to shorten the prototyping period as shown in Fig. 3.

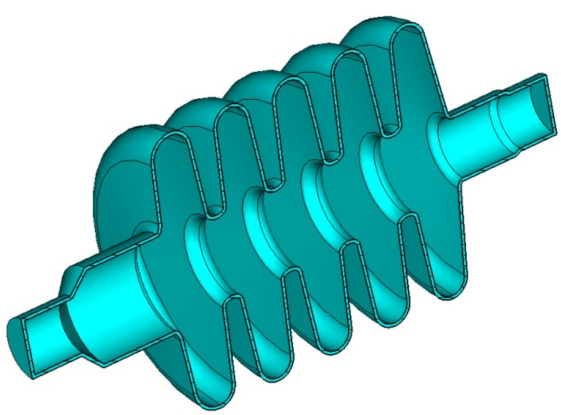

Figure 3: Five-cell prototype cavity.

CAVITY PREPARATION

The cavity fabrication mainly consists of the deep drawing process to make each components and the electron beam welding process to join them in one piece. We made the half cells with the deep drawing process [2].

After deep drawing, we trimmed the equator edge and iris edge to suitable length. In addition, the grooves on the outside wall of the half-cell are machined for welding the stiffening rings. The beam pipe transition parts were also fabricated by using similar deep drawing process.

We etched the surface of each part by using an acidic solution before every electron-beam welding process for better welding performance. The acidic solution consisted of HF, HNO_3 and H_3PO_4 with a volume ratio of 1:1:2. The etching rate was estimated to be about 2.5 μm/min, which was confirmed by several tests using specimens. After etching, each part was cleaned with DI water.

Following the etching, each part was joined by using an electron-beam welding process. Figure 4 shows the five-cell cavity with fixing jigs during the final equator welding step.

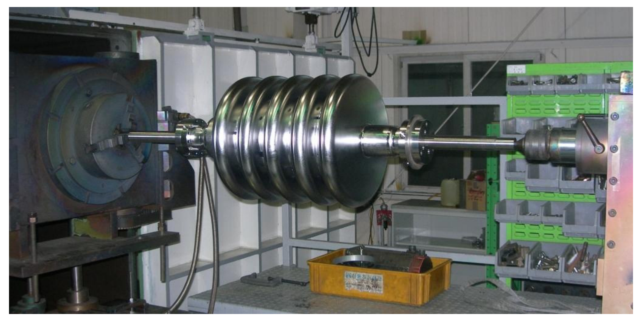

Figure 4: Electron-beam welding of five-cell cavity.

After the cavity fabrication, we tuned the cavity to make the field profile uniform along the beam axis. The field flatness used to express how uniform the field profile is in an N-cell cavity is defined as following [3];

$$\eta_{ff} = \frac{V_{c\max} - V_{c\min}}{\frac{1}{N}\sum_{i=1}^{N} V_{ci}} \times 100\% \cdot \quad (1)$$

Here, V_{ci} is the accelerating voltage of the ith cell. $V_{c\max}$ and $V_{c\min}$ is the maximum and minimum cell voltage in a cavity, respectively. The accelerating voltage in Eq. (1) can be expressed as a phase shift during a bead-pull test.

The initial field measurement result is shown in Fig. 5. The initial field distribution is far from uniform. The fields in the 4th and the 5th cells are almost negligible compared with that in the 1st cell. Before applying the theory-based tuning algorithm, we performed a manual tuning based on the fact that the local field is increased by increasing the local frequency (stretching the cell) and vice versa. By manual tuning, we obtained a field distribution better than the initial profile. Following the manual tuning, we applied the perturbation theory and obtained an almost uniform field distribution after two iterations. The final measurement result is shown in Fig. 6. The final field flatness is uniform within 4%, which is good enough, considering the requirement is about 8%.

The inner surface of the fabricated cavity was treated through the standard buffered chemical polishing (BCP) process and the high pressure rinsing (HPR) process with ultra-pure water. Total material removal was estimated to be about 200 um during the surface treatment.

Figure 5: Initial field distribution.

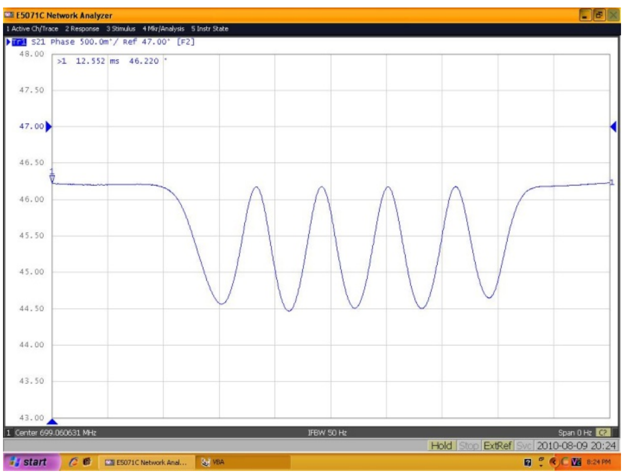

Figure 6: Field distribution after field flatness tuning.

VERTICAL TEST PREPARATION

RF System

The RF system is based on the phase locked loop (PLL) to keep driving the cavity on resonance and to minimize the reflected RF power [4]. The block diagram of the RF system for the vertical test is shown in Fig. 7. A vector signal generator (E4432B, Agilent) is used as VCO (voltage controlled oscillator). A phase comparator that generates a voltage signal proportional to the phase difference between the forward RF power and cavity RF power is used to drive the signal generator frequency modulation function. The output of the phase comparator we used is ranging from 0 V to 2 V according to the phase difference from -180 degree to 0 degree. The voltage offset circuit is used between the phase comparator and the signal generator to match the output of the comparator and the input of the signal generator. For adjusting the initial phase, a trombone-type phase shifter is used due to its large phase shift range (over 360 degrees at 700 MHz).

To build up the accelerating gradient of 8 MV/m in the cavity at 4.2 K without proper magnetic shielding, the required RF power was estimated to be about 1 kW. However, RF amplifier with such a high output power was not available during the test phase. Instead, there are two solid state amplifiers which can provide RF power up to 200 W. Therefore, we designed, fabricated and tested a RF combiner as shown in Fig. 8. The RF combiner is a split coaxial type based on the geometry of 1-5/8 inch rigid coaxial line.

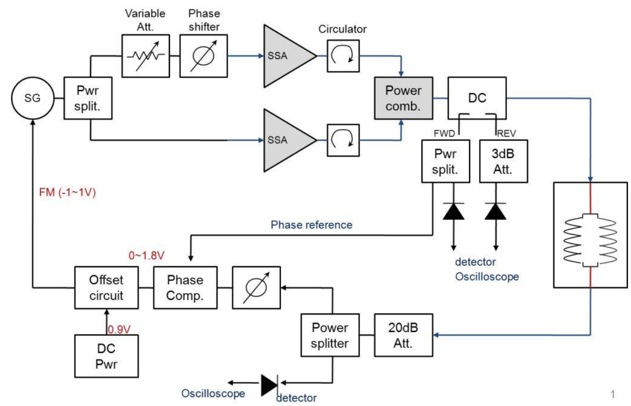

Figure 7: RF System setup for the vertical test.

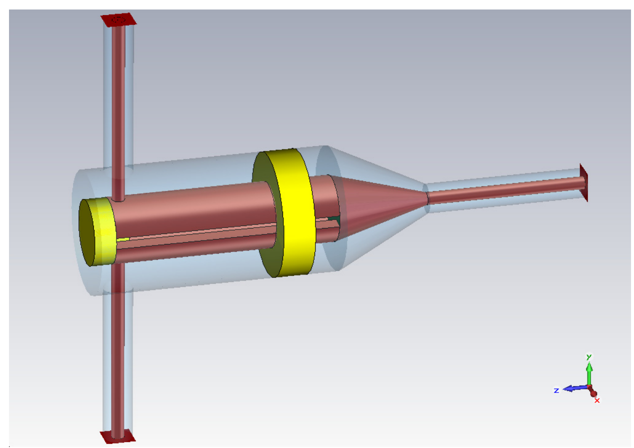

Figure 8: Split coaxial type RF combiner.

The split inner conductor is fixed by using Teflon supporter. The input and output impedance matching was achieved by adjusting the taper region geometry and the gap size at the end of the combiner. Figure 9 shows the fabricated RF combiner. Three type-N connectors were used for the two input ports and one output port. For the RF sealing at end flange, we used a canted coil and indium wire was used at junctions between the electrode and each port.

The fabricated RF combiner was tested at low power level as well as high power level. Figure 10 shows the VSWR of the output port of the RF combiner. Measured S11 parameter is better than -35 dB, which shows good impedance matching. The VSWR is lower than 1.02 at design frequency of 700 MHz and better than 1.05 within ±20 MHz range. The amplitude balance between two input ports was measured to be better than 0.06 dB and phase difference was less than 0.3 degree. Figure 11 shows the high power level test results by using two solid state amplifiers.

Figure 9: Fabricated split coaxial type RF combiner.

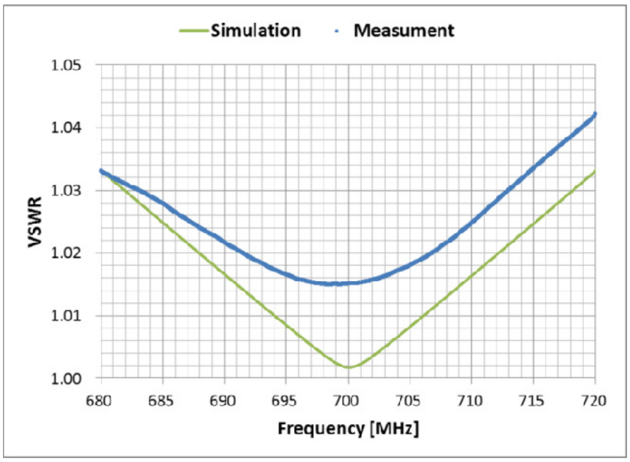

Figure 10: VSWR measurement for the RF combiner.

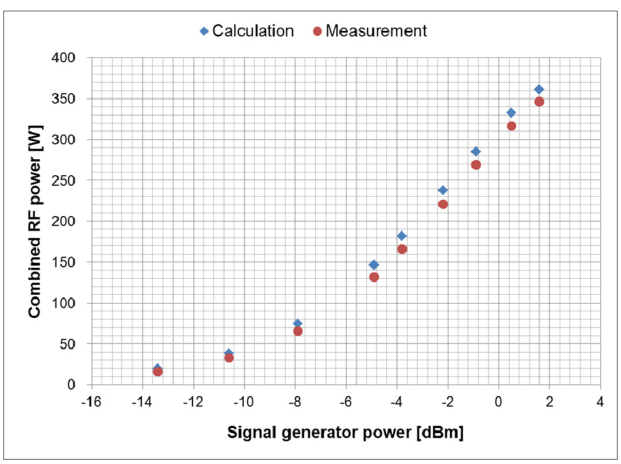

Figure 11: High power performance of the RF combiner.

Cryostat

The height of the cryostat for the vertical test is about 2550 mm and the outer diameter is about 840 mm. The cryostat is double-wall structure and the space between the inner chamber and outer chamber is filled with 40 layers of the super-insulation and evacuated down to 3E-07 Torr. The cryostat system is equipped with a liquid helium level monitor (LM-500, Cryomagnetics) and a temperature monitor (218E, Lake Shore).

Total 10 layers of stainless steel plate of 1 mm thickness are adopted as thermal reflectors. The insert structure with a prototype cavity is shown in Fig. 12.

Figure 12: Insert structure with a prototype cavity.

Radiation Shielding

To shield the radiation during the vertical test, the cryostat was inserted into the concrete pipe with thickness of 95 mm. In addition, the lead plates with 20 mm thickness and the concrete blocks with 400 mm width were installed outside the concrete pipe. The control room was located behind the concrete blocks

TEST RESULTS AND SUMMARY

The overall experimental setup is shown in Fig. 13. For pre-cooling of the cavity, we used liquid nitrogen. Before injection of the liquid helium, the liquid nitrogen is removed by drain and purging with gas helium. The pre-cooling process took about 6 hours from 300 K down to 77 K. The drain and purging process took about 2 hours. It took less than 1 hour to reduce temperature from 77 K to below 5 K. About 350 L of liquid helium was consumed to lower the temperature of the cavity and surrounding structures. Total liquid helium consumption was about 2000 L. Figure 14 shows the temperature variation during the cooling process.

RF power was applied in pulse mode with 250 ms pulsed width and 2 Hz repetition rate (duty factor: 50 %). Figure 15 shows the RF pulse waveforms during the test.

Figure 13: Overall test setup for the vertical test.

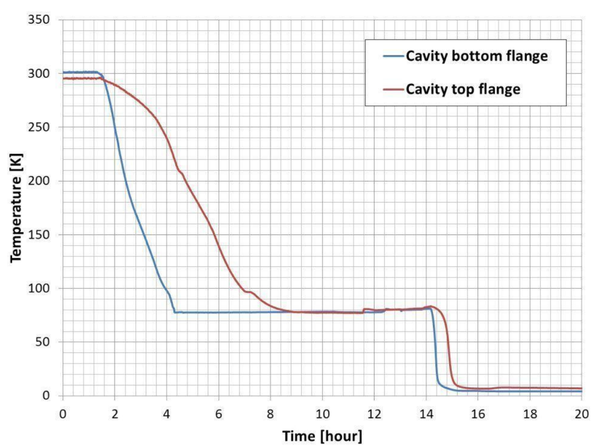

Figure 14: Temperature variation during cooling.

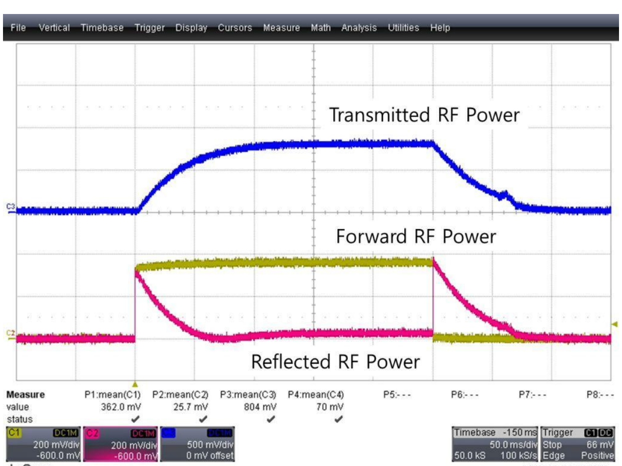

Figure 15: RF pulse waveform during the vertical test.

From the pulse mode measurement, we obtained the unloaded Q as a function of Eacc, as shown in Fig. 16. At a low power level, the measured Q was about 2.9E+8. The BCS resistance at 700 MHz and 4.2 K is about 155 nΩ, and the magnetic resistance is about 126 nΩ at the earth's magnetic field level of 500 mG [3, 9]. If we assume that the additional residual resistance, other than the magnetic resistance, is about 50 nΩ, the total surface resistance is about 330 nΩ, which results in an unloaded Q of about 3.8E+8. From the measured Q, the surface resistance of the cavity is estimated to be about 425 nΩ.

When the accelerating gradient is about 2.7 MV/m, which amounts to a 10 MV/m peak field, the Q value starts to decrease with noticeable increases in radiation level. This decrease may be due to field emission.

The maximum accelerating gradient was 4.2 MV/m with 330 W RF power, which was limited by the available RF power. During the test, we could observe the conditioning effect by noticing the increase of the Eacc and Q value at the same RF input power level. However, the conditioning is considered to be not sufficient due to the limited test time. With enough RF power and sufficient high-power conditioning, we expect the cavity to meet the design accelerating gradient of 8 MV/m.

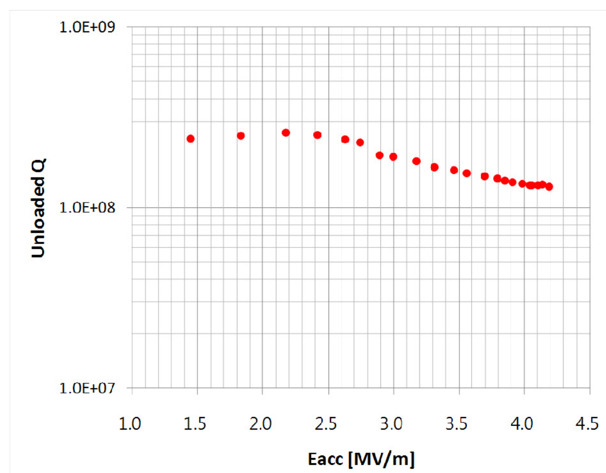

Figure 16: Q0 vs. Eacc for the prototype cavity.

REFERENCES

[1] Sun An, Y. S. Cho and B. H. Choi, "PEFP Low-beta SRF Cavity Design", PAC'07, Albuquerque, 2007.

[2] H. S. Kim, H. J. Kwon, Y. S. Cho and Sun An, "Prototyping and Vertical Test for PEFP Low-beta Elliptical Cavity", SRF2009, Berlin, 2009.

[3] Hasan Padamsee, Jens Knobloch, and Tom Hays, "RF Superconductivity for Accelerators", Wiley-VCH, 2nd Edition.

[4] Tom Powers, "Theory and Practice of Cavity RF Test Systems", SRF'05, Ithaca, 2005.